

Zn–Co Double Metal Cyanides as Heterogeneous Catalysts for Hydroamination: A Structure–Activity Relationship

Annelies Peeters,[†] Pieterjan Valvekens,[†] Rob Ameloot,[†] Gopinathan Sankar,[‡] Christine E. A. Kirschhock,[†] and Dirk E. De Vos^{*,†}

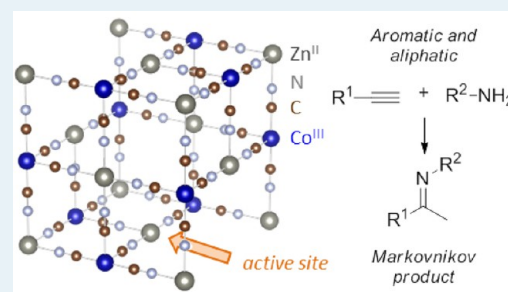
[†]Centre for Surface Chemistry and Catalysis, KU Leuven, Kasteelpark Arenberg 23, 3001 Leuven, Belgium

[‡]Department of Chemistry, University College London, 20 Gordon Street, London WC1H 0AJ, U.K.

Supporting Information

ABSTRACT: Zn–Co double metal cyanide (DMC) materials are effective heterogeneous catalysts for intermolecular hydroaminations. Using the reaction of 4-isopropylaniline with phenylacetylene as a test, the effect of different catalyst synthesis procedures on the catalytic performance is examined. The best activities are observed for double metal cyanides with a cubic structure and prepared with a Zn²⁺ excess, and for nanosized particles prepared via a reverse emulsion synthesis. Detailed study of the active Zn²⁺ sites in the cubic material by EXAFS gives evidence for coordinative vacancies around the Zn, with four cyanide ligands in close proximity of the Zn. The substrate scope of the hydroaminations was successfully expanded to both aromatic and aliphatic alkynes and other aromatic and aliphatic amines. Even with styrenes the reaction proceeded with aromatic amines. The DMC catalysts are truly heterogeneous, possess a high thermal stability and are perfectly reusable.

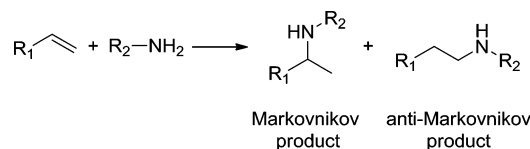
KEYWORDS: amination, zinc, intermolecular, EXAFS, heterogeneous catalysis, alkenes



INTRODUCTION

The one-step amination of alkenes or alkynes, called hydroamination, is a sustainable route to fine chemicals.¹ It is a 100% atom-efficient process without stoichiometric formation of byproducts (Scheme 1). Generally, the reaction can provide two regioisomers, of which the Markovnikov product is thermodynamically favored.¹

Scheme 1. Hydroamination of Alkenes



Furthermore, hydroamination utilizes some of the most readily available carbon sources, while synthesis pathways toward high value amines in industry from alternative starting compounds, such as alcohols, alkyl halides, or carbonyl compounds, overall employ a larger number of steps.^{2,3} The obtained amines, imines, or enamines have widespread applications as bulk chemicals, specialty chemicals or pharmaceuticals. The high activation barriers of hydroaminations however demand the use of efficient catalyst systems. A generic catalyst for both intra- and intermolecular hydroamination of alkyne and alkene feedstock is still lacking. The desire for a heterogeneous system constitutes an additional challenge, and hydroamination research has only scarcely

looked at solid catalysts.¹ Reports exist on metal-cation exchanged zeolites,⁴ clays,^{5,6} and heteropolyacids,^{7–9} and on the Brønsted acid forms of zeolites,^{10–12} clays,¹³ ion exchange resins,^{14,15} and silica gel.¹⁶ Furthermore there are reports on supported (complexes of) Pd,^{17,18} Au,¹⁹ Cu,²⁰ Zn,²¹ V,²² and organolanthanides^{23,24} on solid carrier materials. In most cases, hydroamination is limited to intramolecular reactions or more reactive alkyne substrates or activated alkenes instead of nonactivated alkenes. For materials that contain Brønsted acid sites the activity is limited by protonation of the amine. High temperatures and pressures are needed to counteract this, like in the *tert*-butylamine production with pentasil and β -type zeolites, one of the few commercial applications of hydroamination.²⁵

Recently, our group has shown that double metal cyanides (DMCs) and more in particular Zn–Co DMCs are active heterogeneous catalysts for the hydroamination of phenylacetylene with 4-isopropylaniline.²⁶ DMCs are Prussian blue analogues, which are synthesized by the addition of a water-soluble metal salt (e.g., ZnCl₂) to a water-soluble metal cyanide salt (e.g., K₃[Co(CN)₆]). DMCs are mainly used as catalysts in epoxide polymerization, which is a large scale industrial process.^{27–29} Reactions like the ring-opening polymerization (ROP) of propylene oxide and copolymerization of CO₂ and

Received: December 12, 2012

Revised: February 11, 2013

Published: February 14, 2013

epoxides have received considerable literature attention.^{30–34} While DMCs have been reported to be useful for transesterifications,³⁵ hydrolysis of oils,³⁶ other epoxide ring-opening reactions,³⁷ Prins condensation reactions,³⁸ and synthesis of hyperbranched polymers,³⁹ they remain a generally underexplored class of catalytic materials. Here, we report on a detailed exploration of the substrate scope of DMCs in hydroamination reactions, and we elucidate the relation between structure and activity of the materials. An EXAFS analysis was performed to acquire a detailed insight into the environment of the active Zn sites of the catalyst. This technique gives detailed local information, which is crucial for understanding the structure–activity relationship.

RESULTS AND DISCUSSION

Synthesis and Characterization of Zn–Co DMCs. Zn–Co DMC catalysts were prepared by various synthesis techniques, as described in the Experimental Section. An overview of the relevant synthesis parameters is given in Table 1. The Zn(II)–Co(III) catalysts in this paper are typically

Table 1. Overview of Synthesis Parameters of Prepared Zn–Co–DMCs

| catalyst | Co-CA | CA | Zn source |
|--------------|---------------|-------------------|---|
| DMC-PTMEG | PTMEG | ^t BuOH | ZnCl ₂ |
| DMC-PEG | PEG | ^t BuOH | ZnCl ₂ |
| DMC-P123 | P123 | ^t BuOH | ZnCl ₂ |
| DMC-X | – | ^t BuOH | ZnCl ₂ |
| DMC-pure | – | – | ZnCl ₂ |
| DMC-1:1 | – | – | ZnCl ₂ |
| DMC-sulfate | PTMEG | ^t BuOH | ZnSO ₄ ·7H ₂ O |
| DMC-triflate | PTMEG | ^t BuOH | Zn(CF ₃ SO ₃) ₂ |
| NDMC-Igepal | Igepal CA-520 | ^t BuOH | ZnCl ₂ |

synthesized by the addition of an excess of ZnCl₂ to K₃[Co(CN)₆], but other possible metal combinations are Cu(II)–Co(III), Zn(II)–Fe(II), Zn(II)–Fe(III), Cu(II)–Fe(II), Ni(II)–Co(III), etc. Additives have been proposed to make the DMCs more active. A complexing agent (CA), often an alcohol like *tert*-butanol (^tBuOH), is used alongside cocomplexing agents (co-CA) which are polyethers like poly(tetramethylene ether) glycol (PTMEG), polyethylene glycol (PEG) or Pluronic P123 (containing polyethylene glycol and polypropylene glycol segments, P123). The role of these complexing agents is multifold, but they are believed to affect the active site accessibility and particle size of the DMCs by coordinating on peripheral metal cations and simultaneously acting as protecting agents.³³ DMC-PTMEG, DMC-PEG, and DMC-P123 were prepared analogously, but with different co-CAs, while DMC-X was prepared with only ^tBuOH, in the absence of a co-CA. For DMC-pure, no alcohol additives were used at all. This is also the case for DMC-1:1, but here the ratio of zinc to cobalt in the synthesis mixture was 1:1, while mostly a Zn/Co ratio of 10:1 was applied. To investigate the influence of the anion of the used zinc salt, ZnCl₂ was replaced by ZnSO₄·7H₂O and Zn(CF₃SO₃)₂, resulting in DMC-sulfate and DMC-triflate, respectively.

A higher hydroamination activity is expected for small particles.²⁶ Smaller particle size can be obtained by using a reverse emulsion technique, in which an aqueous phase is dispersed in a cyclohexane phase.⁴⁰ Igepal CA-520, a

polyoxyethylene isooctylphenyl ether type surfactant, is used both as a surfactant for stabilizing the aqueous droplets and as co-CA (NDMC-Igepal, with N = nano).

The structure of the DMCs is, despite extensive research for epoxide polymerization, still a matter of debate. The [Co(CN)₆]^{3–} anion and the Zn²⁺ cations build a structure which is terminated by the complexing agents, or by water molecules. Some preliminary characterization of some materials were already reported before,²⁶ and relevant data were selected to illustrate the properties of these materials. X-ray powder diffraction analysis was performed on the DMC samples (Figure 1). This shows that all DMC samples are crystalline. Most show reflections at 14.9°, 17.1°, 24.3°, 34.8°, and 39.1° 2θ, typical of a cubic lattice structure with space group *Fm3m*, as was described by Mullica et al.⁴¹ DMC-PTMEG, DMC-P123 and NDMC-Igepal display the most pronounced phase purity of the cubic phase. However, additional lines were observed for several materials, for instance when PEG was used as the co-CA, or when Zn compounds other than ZnCl₂ were used. Reflections at 14.5°, 17.0°, 20.6°, 23.7°, and 24.7° 2θ are readily assigned to the monoclinic phase with space group *P11m*, as described by Wojdel et al.⁴² Despite the close overlap of some of the lines arising from the two different phases, the observation of reflections at e.g. 20.6° and 23.7° 2θ is clearly diagnostic for the presence of the monoclinic phase. The relation between the 3D structure of the DMC materials and their catalytic activity will be addressed in detail below (vide infra).

Selected SEM images of DMC-PTMEG, DMC-pure and NDMC-Igepal show that the synthesis procedure affects particle size, morphology and particle size distribution of the catalyst to a great extent (Figure 2). Comparison of DMC-PTMEG and DMC-pure, both synthesized via the standard procedure, shows the importance of using complexing agents. DMC-pure shows large crystalline particles, many of which present a morphology of truncated octahedra, consistent with the cubic symmetry. In contrast, DMC-PTMEG displays smaller but highly coagulated and nonuniform particles. The SEM image of NDMC-Igepal however shows very small, uniformly sized particles. This indicates that the reverse emulsion technique indeed allows for a more controlled and fine particle size of the DMC material.

Pyridine adsorption followed by infrared (IR) spectroscopy was performed on NDMC-Igepal. Figure 3 shows the difference spectrum of NDMC-Igepal before and after adsorption of pyridine. The IR bands at 1610 and 1451 cm^{–1} prove the presence of Lewis acid sites, while Brønsted acid sites are absent, as indicated by the absence of peaks at 1639 and 1545 cm^{–1}.⁴³ This shows that Zn–Co DMCs are strictly Lewis acid solid catalysts. The catalytically active Lewis acid sites are presumed to be associated with Zn sites in the DMC structure.³⁷ Further evidence for this will be given below.

As some of the hexacyanocobaltate anions are missing in the cubic structure due to charge considerations (vide infra), the structure has substantial porosity, giving rise to high internal surface areas. The porous framework has voids of about 8.5 Å, but they are connected through small windows of only about ~4.2 Å diameter.⁴⁴ In view of these properties, double metal cyanides have been studied for hydrogen storage and also for light alkane separations, etc.^{45,46} An indication of the pore size can be obtained by performing nitrogen sorption on the DMC samples. Horvath–Kawazoe (HK) pore size estimations yielded average values of about 4.8 Å. However, as most reactants for

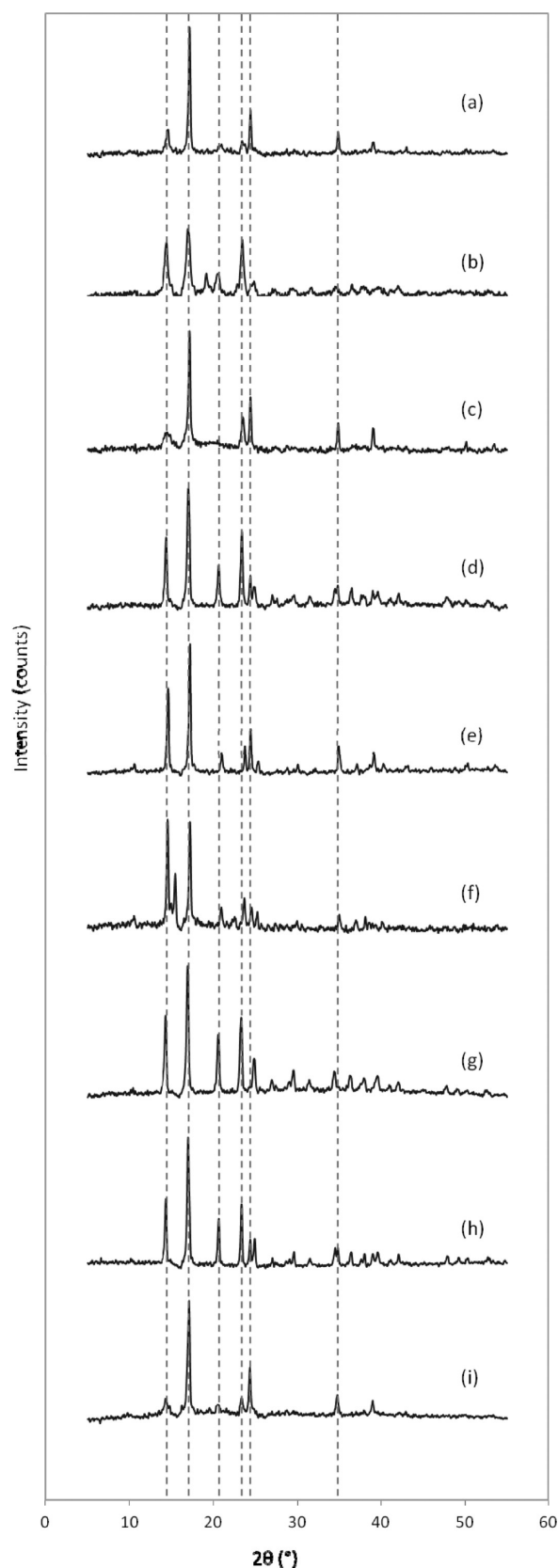


Figure 1. X-ray diffractograms of synthesized DMC catalysts: (a) DMC-PTMEG, (b) DMC-PEG, (c) DMC-P123, (d) DMC-X, (e) DMC-pure, (f) DMC-1:1, (g) DMC-sulfate, (h) DMC-triflate, and (i) NDMC-Igepal.

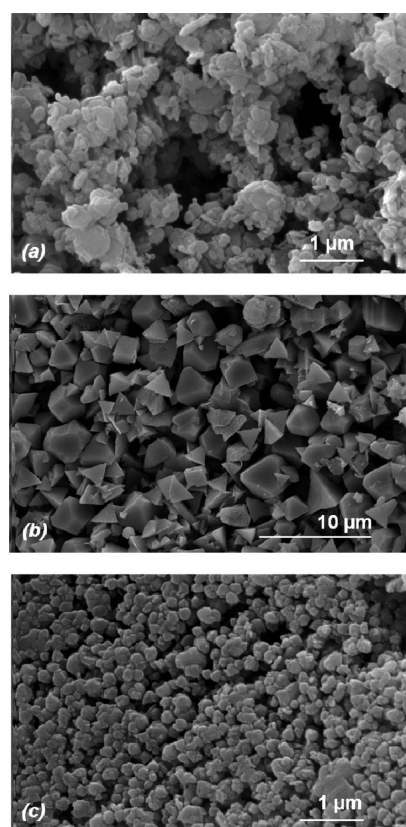


Figure 2. SEM images of (a) DMC-PTMEG, (b) DMC-pure, and (c) NDMC-Igepal. Reproduced with permission from ref 26. Copyright 2011 The Royal Society of Chemistry.

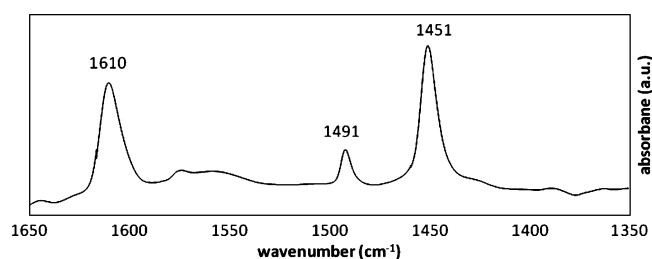


Figure 3. IR difference spectrum: Subtraction of absorbance before and after adsorption of pyridine to NDMC-Igepal. Pyridine was adsorbed at 323 K (25 mbar); spectrum was recorded after evacuation at 448 K.

the hydroaminations contain aromatic rings, they are expected to react mainly on the outer particle surface. The nitrogen sorption isotherms obtained are shown in Figure 4, for a standard material (DMC-PTMEG) and for NDMC-Igepal prepared in a reverse emulsion. BET surface areas of respectively 464 and 552 m²/g were obtained. For NDMC-Igepal, the steeper rise of the isotherm at intermediate relative pressures is indicative of a larger external surface area, in accordance with the smaller overall particle size of this material.²⁶

Thermogravimetric analysis of the DMCs was performed under oxygen flow. The weight loss and its derivative as a function of the temperature are shown in Figure 5 for DMC-PTMEG, DMC-pure, DMC-X, and NDMC-Igepal as representative materials. All of them show a very sharp mass decay when the cyanide ligands are burned off. TGA analysis also

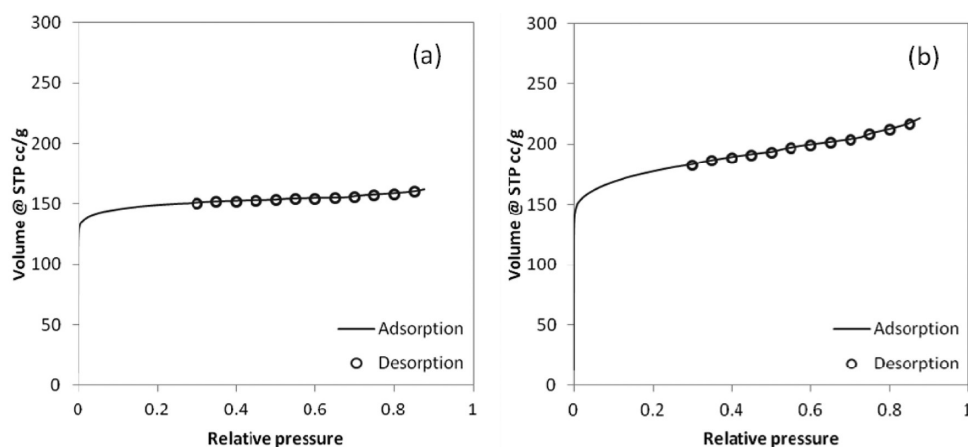


Figure 4. Nitrogen sorption isotherms (77 K) of (a) DMC-PTMEG and (b) NDMC-Igepal.

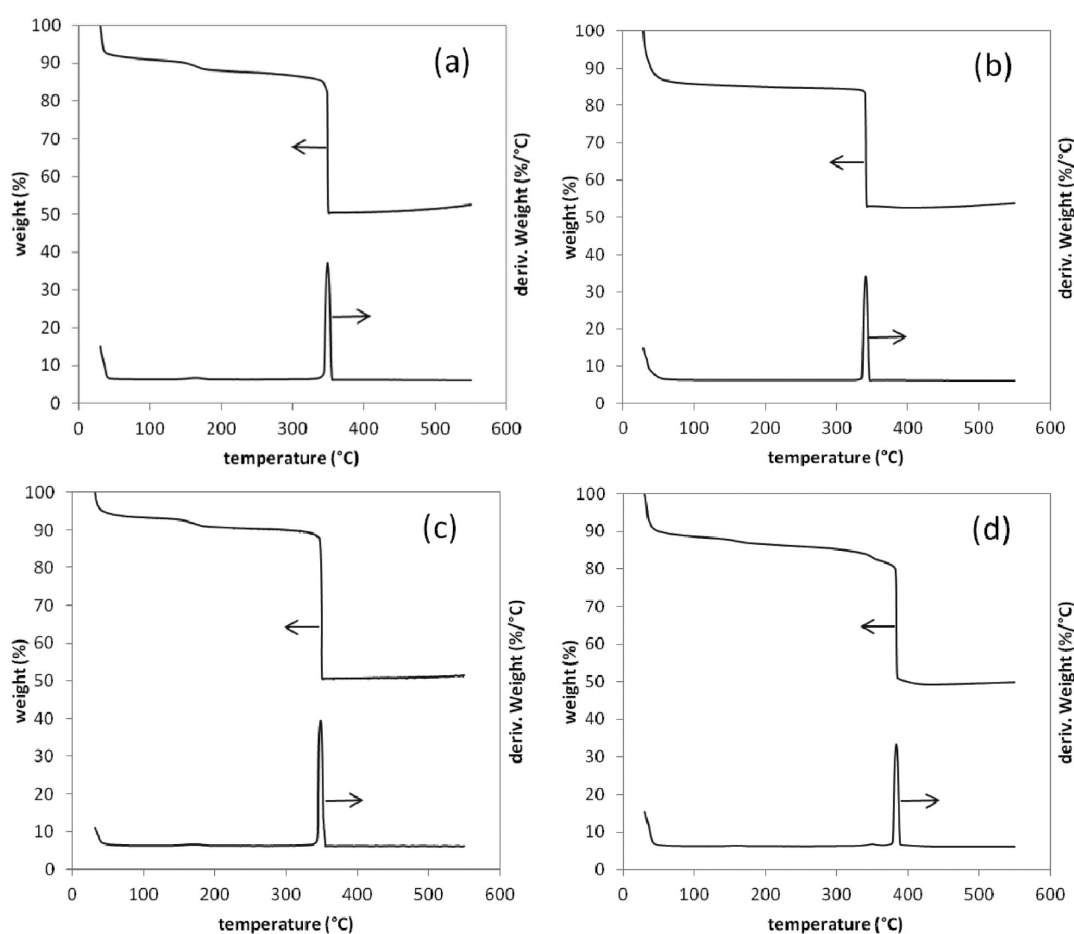


Figure 5. TGA and DTGA profiles for (a) DMC-PTMEG, (b) DMC-pure, (c) DMC-X, and (d) NDMC-Igepal.

shows that physisorbed water is removed fast in a first stage (<100 °C), followed by removal of ^tBuOH, the co-CA and finally the cyanide ligands, which under oxidizing conditions are removed as (CN)₂.⁴⁷ At this stage the Zn–Co cyanide salt is converted to the corresponding oxides Co₂O₃ and ZnO, which is known as Rinmann's green, and is easily recognized by the dark green color.⁴⁸

Elemental analysis was performed with EDX (Figure 6). The Zn/Co/Cl molar ratio calculated is 1.85:1:0.03, for DMC-PTMEG, meaning that the Zn:Co ratio is slightly higher than the stoichiometrically expected 1.5. The low chlorine content

indicates there are hardly traces of ZnCl₂ left. In view of the excess of Zn²⁺ in the synthesis mixture and in the structure, it is expected that zinc terminates the crystals and is abundant on the outer surface.

Catalytic Activity and Substrate Scope. To probe the catalytic activity of the different DMC catalysts, a test reaction was used. The hydroamination of 4-isopropylaniline **1** and phenylacetylene **2** results in the formation of the enamine hydroamination product (Scheme 2), which further tautomerizes to the thermodynamically more stable imine product (4-isopropylphenyl)(1-phenylethylidene)amine **3**. The reaction

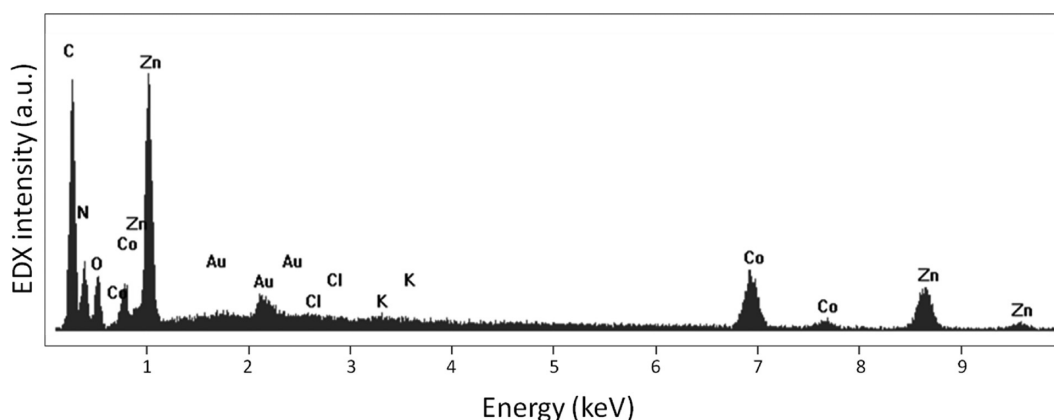
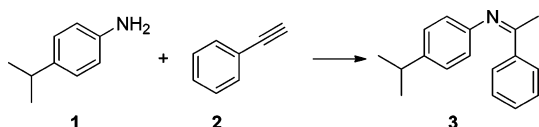


Figure 6. EDX analysis of Zn–Co–DMC–PTMEG. Note that the Au signal originated from Au sputtering on the sample for conductivity.

Scheme 2. Test Reaction: Hydroamination of Phenylacetylene with 4-Isopropylaniline



was conducted at 383 K for 24 h in the presence of the DMC catalyst in toluene solvent. All reactions resulted in the Markovnikov-type addition product, as expected for Lewis acidic catalysts.¹ For detailed experimental procedures and characterization of products, see Supporting Information.

Earlier, we reported that Zn(II)–Co(III) catalysts were the most active DMCs, while Zn(II)–Fe(II), Zn(II)–Fe(III), Cu(II)–Fe(II), and Cu(II)–Co(III) showed negligible catalytic activity in the hydroamination test reaction.²⁶ Table 2 lists

Table 2. Hydroamination Yields (%) of 3 Obtained with Different Zn–Co-Based DMC Catalysts^a

| entry | catalyst | yield (%) ^b |
|-------|--|------------------------|
| a | DMC-PTMEG | 92 |
| | | 92 ^c |
| b | DMC-PEG | 18 |
| c | DMC-P123 | 67 |
| d | DMC-X | 79 |
| e | DMC-pure | 40 |
| f | DMC-sulfate | 8 |
| g | DMC-triflate | 28 |
| h | NDMC-Igepal | 96 |
| i | ZnCl ₂ ^d | 0 |
| j | K ₃ [Co(CN) ₆] ^d | 0 |

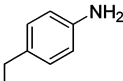
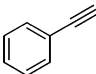
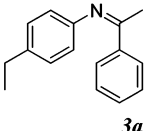
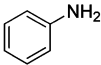
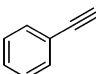
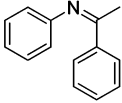
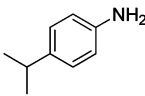
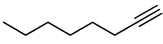
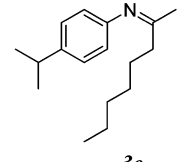
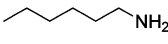
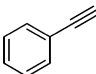
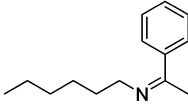
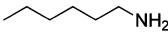
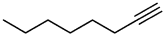
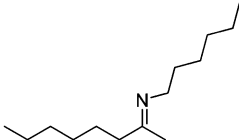
^aConditions: 1 mmol of 4-isopropylaniline and 0.5 mmol of phenylacetylene with 50 mg of catalyst in 1 mL of toluene. Reactions were carried out at 383 K for 24 h. ^bCalculation of yield based on phenylacetylene, GC yield. ^cYield of hydroamination product after third consecutive run. ^d5 mol % of the metal salt (with respect to phenylacetylene) was added.

the hydroamination yields for the DMC catalysts as well as for their metal salt precursors. Poly(tetramethylene ether) glycol (PTMEG) was found to be one of the most suitable co-CAs, with the Pluronic coblock polymer (P123) based material being somewhat less active (Table 2, entries a and c). A low activity was found for the polyethylene glycol (PEG) containing material (entry b). These trends coincide with the structural

features as evident from Figure 1 a–c: the best activities are found for nearly phase-pure cubic materials. While the reason for the poor results with PEG is not immediately clear, it should be noted that the molecular weight (MW) of the PEG used (2000 g/mol) is significantly higher than that of the PTMEG (1000 g/mol). The presence of the PTMEG co-CA also has a beneficial effect on the hydroamination activity in comparison with DMC-X, prepared without any co-CA (Table 2, entry d vs a). Finally, omission of the CA ^tBuOH resulted again in a low hydroamination activity, which in this case can be related to the low outer surface area available for catalysis (entry e). NDMC-Igepal, prepared by the reverse emulsion technique, was the most active DMC material. Again, the high activity seems to be connected to the cubic structure, combined in this case with a large outer surface (entry h).

Assuming that the zinc sites of the Zn–Co DMC-PTMEG material are the active sites for the hydroamination reactions, the choice of the Zn salt for catalyst preparation may affect the catalytic activity. The nature of the zinc precursor was indeed found to have a large influence: sulfate- or triflate-based Zn salts resulted in DMCs with much lower hydroamination activities (Table 2, entries f and g vs a). In first approximation, this anion effect can again be traced back to the phases formed: the cubic phase is the predominant one formed in the presence of ZnCl₂, while significant fractions of side phases are present when other precursors are employed (Figure 1a, g, and h). This is in agreement with literature; Huang and co-workers also found an effect of the metal salt precursor on the structure of the DMC.³⁰ Only with ZnCl₂ a cubic structure was obtained, while with ZnSO₄ and Zn(CH₃COO)₂ a different phase was formed. For polymerization of propylene oxide only the cubic form was highly effective, while the others had a low activity.³⁰ On the other hand, it cannot be excluded that some chloride ions would remain coordinated to the Zn²⁺ in the final catalyst. However, from EDX measurements (Figure 6) it can be concluded that this amount of Cl[−] on the surface is only a trace. As ZnCl₂ clearly plays a crucial role in the catalyst preparation, the catalytic activity of ZnCl₂ was also tested as such, even if ZnCl₂ is only partially soluble in the reaction conditions. However, no hydroamination products were found (entry i), indicating that the dispersed, coordinated zinc sites in Zn–Co DMCs are essential for activity. K₃[Co(CN)₆] was equally inactive (entry j). This shows that the catalytic activity of the DMCs is not merely a summation of the catalytic effect of the respective metals, but results from the unique structure of the

Table 3. Hydroamination Yields (%) Obtained with Different Amines and Alkynes^a

| entry | Amine | Alkyne | Product | Yield (%) ^b |
|-------|---|---|--|------------------------|
| a |  |  |  3a | 88 |
| b |  |  |  3b | 79 |
| c |  |  |  3c | 70 |
| d |  |  |  3d | 5 48 ^c |
| e |  |  |  3e | 5 46 ^c |

^aConditions: 1 mmol of amine and 1 mmol of alkyne with 50 mg of NDMC-Igepal catalyst in 1 mL of toluene. Reactions were carried out at 423 K for 24 h. ^bCalculation of yield based on amine, GC yield. ^c0.5 mmol of amine instead of 1 mmol and reaction at 473 K.

DMC and the influence of this structure on the properties of the Zn²⁺ ion.

For DMCs in epoxide polymerization, it has been found that a ZnCl₂ excess with respect to K₃[Co(CN)₆] in the synthesis beneficially affects the activity. In DMC literature this is often attributed to the higher activity of a less crystalline material, and the use of a co-CA is supposed to have a similar effect.^{31,32} However, our data do not indicate that the most active materials have a decreased crystallinity. Rather, both the ZnCl₂ excess and the CAs result in materials with small particle size, with Zn preferably located on the external surface. XRD patterns show that both the 1:1 material and the DMC prepared with an excess of ZnCl₂ display sharp peaks (Figure 1, entry e and f). While most catalysts presented in Table 1 were prepared with a 10:1 Zn:Co ratio, the material prepared using a 1:1 Zn:Co ratio in the synthesis was also tested. This resulted in an activity decrease by more than 20%, suggesting that Zn cations terminating the lattice at the external surface play an important role in the catalysis.

NDMC-Igepal, prepared by the reverse emulsion technique, yielded very small, uniform and phase pure particles which showed the highest activity obtained so far. These were employed in further experiments to expand the substrate scope of the catalyst. Table 3 shows the hydroamination yields of aromatic and aliphatic amines with both aromatic and aliphatic alkynes. The reactions were conducted with equimolar amounts of amine and alkyne at 423 K for 24 h. From entries a and b it

appears that an electron donating substituent in the para position of the aniline results in higher hydroamination yields. These substituents make the amine more nucleophilic for attack on the alkyne moiety. In entries c, d, and e, an aliphatic amine or alkyne is used as substrate. The hydroamination of 1-octyne with 4-isopropylaniline (Table 3, entry c) proceeds smoothly with the NDMC-Igepal catalyst. Aliphatic amines appear to be more difficult reactants. Reacting 1-hexylamine with phenylacetylene at 423 K, a yield of only 5% was obtained (entry d). However, when working with an excess of the phenylacetylene at 473 K this yield was raised to 48%. At this temperature there was however a significant byproduct formation because of phenylacetylene oligomerization. Also with 1-octyne a 46% yield of the hydroamination product could be obtained (Table 3, entry e). Heterogeneous catalysts that can catalyze the intermolecular reaction of aliphatic alkynes with aromatic amines have been reported, but aliphatic amines have till now only rarely been used successfully. This indicates that DMCs are general and versatile catalysts for alkyne hydroaminations.

While the results with alkynes are encouraging, the intermolecular hydroamination of olefins in mild reaction conditions remains challenging. Therefore, a range of styrenes were tested in the hydroamination with anilines (Table 4). Again reactions were conducted at 423 K for 24 h. Promising results were obtained with 4-methoxy and 4-ethoxystyrene. When working with 0.5 mmol of 4-isopropylaniline instead of 1

Table 4. Hydroamination Yields (%) Obtained with Different Anilines and Styrenes^a

| entry | Aniline | Styrene | Product | Yield (%) ^b |
|-------|-----------|---------|---------|----------------------------------|
| f | | | | 8 |
| g | <i>1</i> | | | 10 27 ^c |
| h | <i>1</i> | | | <1 |
| i | | | | 30 ^d (ratio 1:1) |
| j | <i>1a</i> | | | 14 ^d (ratio 1:1.3) |

^aConditions: 1 mmol of aniline and 1 mmol of styrene with 50 mg of NDMC-Igepal catalyst in 1 mL of toluene. Reactions were carried out at 423 K for 24 h. ^bCalculation of yield based on amine, GC yield. ^c0.5 mmol of aniline instead of 1 mmol. ^dCombined yield.

mmol, a 27% yield could be obtained with 4-methoxystyrene. The lower concentration of the amine probably facilitates coordination of the styrene to the active Lewis acid sites, giving a higher hydroamination yield. This is in line with literature findings on hydroamination by late transition metals. For Zn²⁺ ion exchanged Beta-zeolite, Penzien et al.⁴ suggested that the mechanism comprises a nucleophilic attack of the amine on the metal-coordinated unsaturated bond. This coordination makes the π -system susceptible for attack by a nucleophile.

In comparison with the unsubstituted styrene, the hydroamination yield is higher with electron donating substituents in the para position (Table 4, entries f, g, and h). When a styrene with an electron withdrawing substituent in this position was tested, such as 4-bromostyrene (not shown), no hydroamination product was formed at all, indicating that an increased electron density on the styrene double bond enhances the hydroamination rate. This may indicate that a sufficient electron density, as provided by alkoxy substituents, is required to allow coordinative bonding of the double bond on the Zn sites. With the sterically demanding 2,4,6-trimethylstyrene only very little hydroamination product was obtained (<1%), just like for 4-*tert*-butyl styrene (<1%). When 4-isopropylaniline was replaced with aniline, good yields were

obtained, but next to the hydroamination product also the hydroarylation product was retrieved (Table 4, entries i and j).

Further tests show that Zn–Co DMCs are stable recyclable heterogeneous catalysts. This was demonstrated by a hot filtration test, a recycling test and structure analysis. In the hot filtration test a reaction mixture was prepared analogously to the conditions used in Table 2 with DMC-PMEG catalyst. A sample was taken after 2 h of reaction and filtered without cooling. The resulting filtrate was left stirring for an additional 4 h and no further catalytic conversion was observed, indicating that no active species leach from the heterogeneous catalyst. DMC-PTMEG also kept its high activity after three consecutive runs (see Table 2, entry a), indicating that it is a stable and recyclable catalyst.

Figure 7 shows the X-ray diffractograms of NDMC-Igepal before reaction and after reaction at 383, 423, and 473 K. This clearly demonstrates that the structure of the catalyst is preserved at the first two reaction temperatures. However, at the high reaction temperatures of 473 K, changes in the catalyst structure occur after 24 h, which is most likely due to prolonged contact with solvent or reactants at this reaction temperature. We can therefore conclude that NDMC-Igepal is a stable catalyst up to the reaction temperature of 423 K.

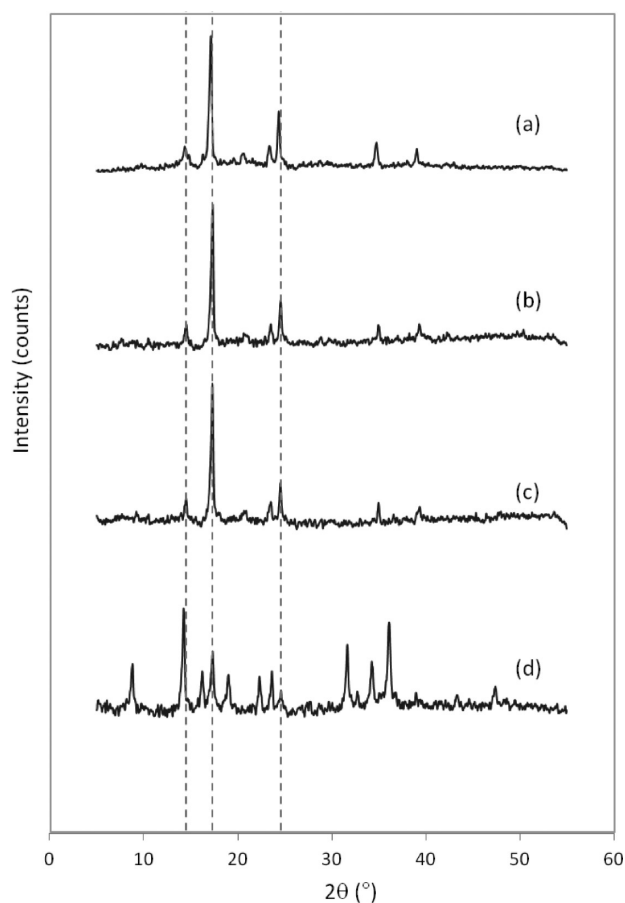


Figure 7. X-ray diffractograms of NDMC-Igepal before reaction (a), after reaction at 383 K (b), after reaction at 423 K (c) and after reaction at 473 K (d).

Structure–Activity Relationship. So far, the most active catalytic materials all display a cubic crystal structure with substantial phase purity. The cubic $Fm\bar{3}m$ model as proposed by Mullica et al. demands vacancies in the octahedral lattice due to the unequal charge of the hexacyanocobaltate anion $[\text{Co}(\text{CN})_6]^{3-}$ and the Zn^{2+} cation, which creates open coordination sites associated with Zn.⁴¹ In the monoclinic phase however, Zn is tetrahedrally coordinated and no free coordination sites are encountered.⁴²

Materials with high phase purity were prepared for further investigation. For the cubic structure a procedure described by Kuyper and Boxhoorn was followed without addition of complexing agents.⁴⁹ The X-ray diffractogram of this material is shown in Figure 8a and is compared with the cubic structure model based on Mullica et al.⁴¹ (Figure 8, b), which confirms that the material is purely cubic. Subsequently, an attempt was made to prepare a material with a high content of the monoclinic side phase. This was accomplished with a lower Zn/Co ratio and the use of zinc sulfate instead of zinc chloride as Zn source.^{45,50} The X-ray diffractogram is shown in Figure 8c. Reflections at 20.6° and 23.7° 2θ together with high intensity of the reflection at 14.5° 2θ are diagnostic for the monoclinic phase.

When comparing the activity of these materials with high phase purity for the test reaction of **1** and **2**, it was again found that the cubic form was the best catalyst. The yield of the hydroamination product **3** could be almost doubled with the cubic form rather than using the material with a high fraction of

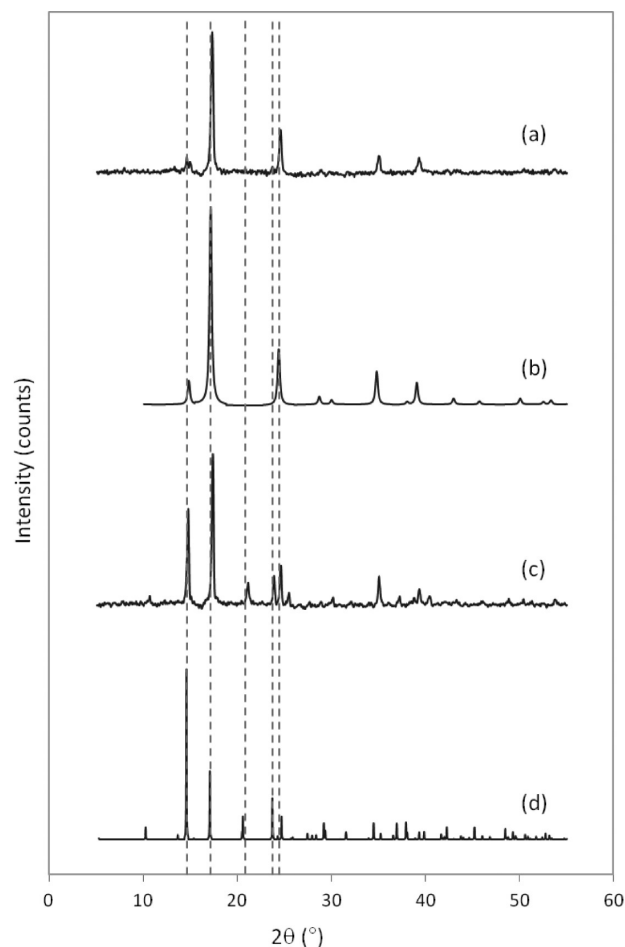


Figure 8. X-ray diffractograms of Zn–Co DMC samples: (a) highly cubic material, (b) simulated model of a cubic Zn–Co DMC according to Mullica et al.,⁴¹ (c) highly monoclinic synthesized material, and (d) simulated model of a monoclinic Zn–Co DMC according to Wojdel et al.⁴²

the monoclinic side phase (82% vs 42%). This is another indication of the higher activity of a cubic phase in comparison with the monoclinic side phase.

The cubic DMC of Figure 8a was characterized by EXAFS. From a detailed study of both the Co-edge and Zn-edge data, the environments of the Co ions and the active Zn sites can be described more precisely. The results of the Co-edge EXAFS analysis are presented in Figure 9. The Fourier transformed data fit very well with the proposed cubic model for the first two coordination shells around Co: six carbon atoms can be fitted at a distance of 1.90 Å and further 6 nitrogen atoms at 3.00 Å. The high intensity of the second shell is due to the linear arrangement of the cyanide ligand; a Co–C–N bond angle of 180° enhances forward scattering and results in high intensities of the radial distribution curve. This confirms that the hexacyanocobaltate anions are incorporated in intact octahedral coordination geometry in the structure of the catalyst; cobalt is fully coordinated, leaving no sites for catalysis. The intact 6-fold coordination of cobalt in the DMC complex is supported by the strong bonding nature of the CN^- ligand; strong σ -donation and π -backbonding result in a stable complex. In this context the hexacyanocobaltate anion plays a role of structure builder by placing the cyano-ligands in exactly

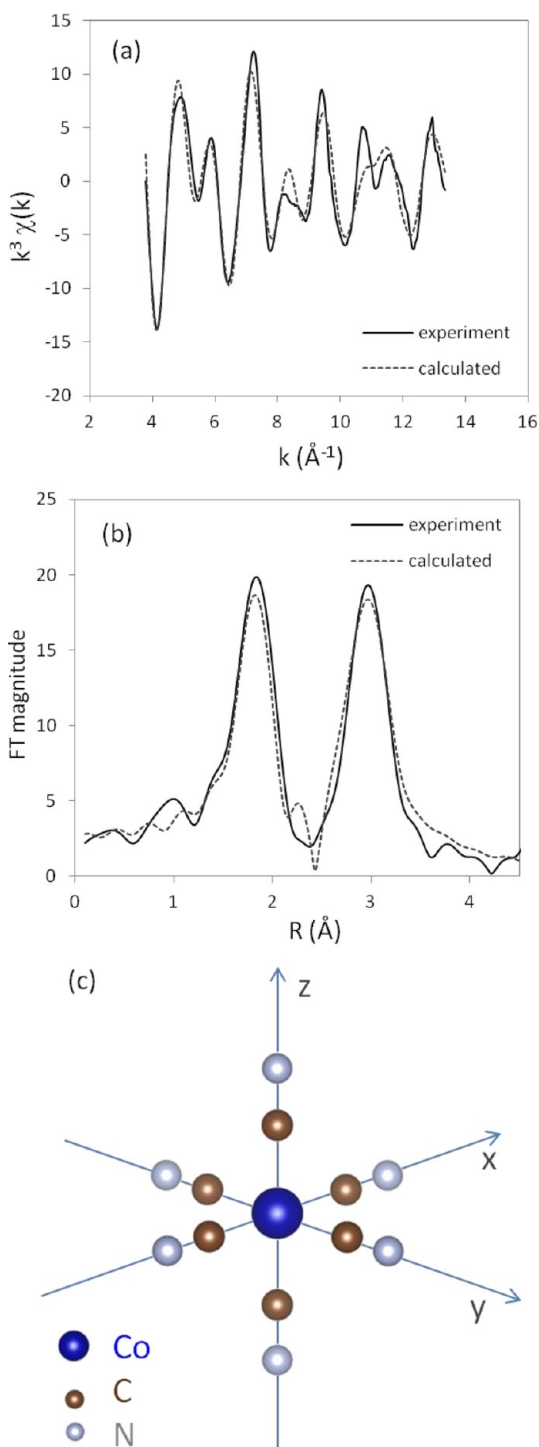


Figure 9. Co–K-edge data: (a) k^3 -weighted raw EXAFS data, (b) Fourier transform fit, and (c) local environment around Co in the Zn–Co DMC structure.

the right position in the double metal cyanide complex to allow catalysis at the Zn-sites.

The Zn-edge data are shown in Figure 10. While Zn should be in an octahedral site, according to the cubic model, the structure should contain a large number of hexacyanocobaltate vacancies due to the charge neutrality of the system. This would lower the actual coordination number around Zn from 6 to an average of 4. The observed average $Fm\bar{3}m$ structure implies a random distribution of these vacancies throughout the lattice.

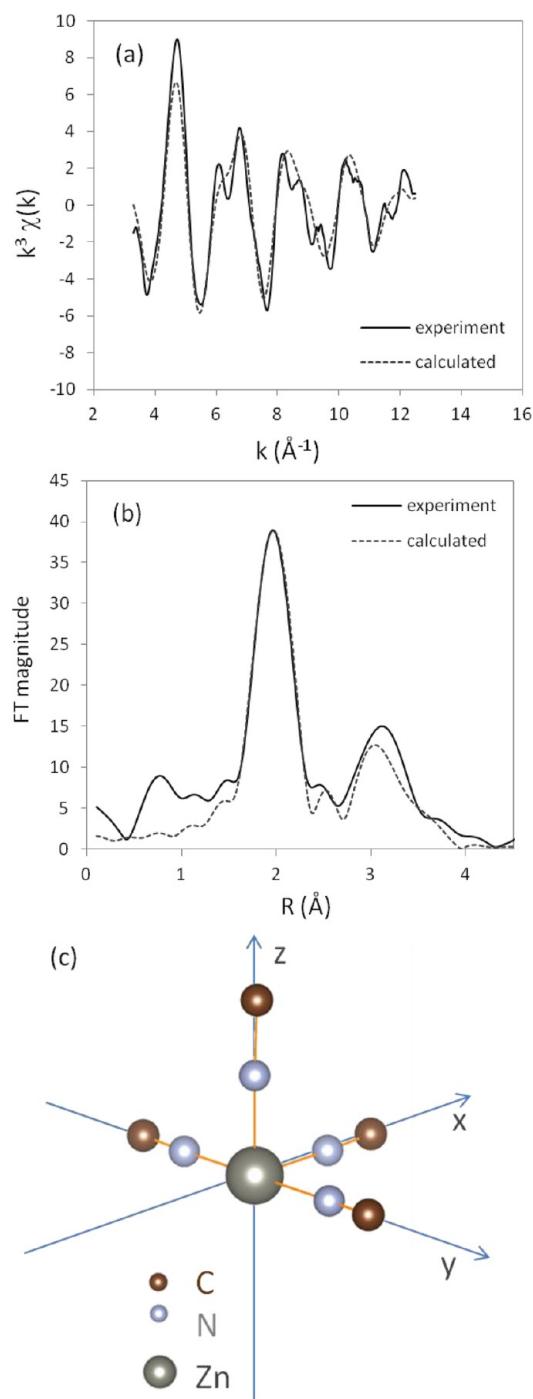


Figure 10. Zn–K-edge data: (a) k^3 -weighted raw EXAFS data, (b) Fourier transform fit, and (c) local environment around Zn in the Zn–Co DMC structure. Four ligands are located in close proximity, while a fifth neighbor is at a nonbonding distance (not shown).

This means that the number of nitrogen neighbors around Zn can theoretically vary between 2 and 6. EXAFS data indeed demonstrate that the number of neighbors around Zn is well below 6. A few feasible structure models were tested and a satisfactory fit was obtained with 4 nitrogen neighbors in close proximity to the Zn, even if models with 5 or 3 nitrogen neighbors also appeared possible. The best fit obtained is shown in Figure 10c in which 4 nitrogen neighbors are present at a close distance of 1.98 Å and a fifth neighbor is further away

at a nonbonding distance of 2.48 Å, resulting in the small shoulder visible in the Fourier transform radial distribution.

This model is based on the unsymmetrical environment of the ligands around zinc in an incompletely coordinated octahedral position which lacks an inversion center. As the material was prepared without any CAs or co-CAs, and was vacuum dehydrated prior to EXAFS analysis, the Zn in the dehydrated cubic material probably adopts a pseudotetrahedral coordination, in which it is moving slightly out of its position in the octahedral lattice. This implies that the angle of the Zn–N bonds is not 180° as proposed from the diffraction based model, but is locally distorted. This results in smaller Zn–N distances compared to the cubic crystallographic model of Mullica et al. (1.96 vs 2.09 Å) while a fifth neighbor is at a larger distance (2.48 vs 2.09 Å). This EXAFS study confirms that free coordination sites exist, which allow the Zn cations to function as Lewis acid catalytic sites.

CONCLUSION

Zn–Co double metal cyanides are excellent catalysts for a wide range of intermolecular hydroamination reactions, particularly using alkynes. They are easily prepared, stable, reusable and truly heterogeneous. The high activity of the material is ascribed to Lewis acid zinc sites; typically the Zn is in a pseudo-octahedral environment, but instead of 6, only 4 or 5 cyanide ligands surround the Zn, as shown by an EXAFS study. Although double metal cyanides are underexplored in heterogeneous organic catalysis, these catalysts offer a high potential for many applications because of the high level of possible variation in e.g. active metals, particle size, morphology and hence activity.

EXPERIMENTAL SECTION

General Procedure for the Synthesis of Zn–Co DMC Catalysts. *Standard DMCs.*³³ Solution A is prepared by dissolving 10 mmol of a metal salt (ZnCl₂, ZnSO₄·7H₂O (DMC-sulfate) or Zn(CF₃SO₃)₂ (DMC-triflate)) in 100 mL of deionized water. To this solution, 1 mmol of cocomplexing agent (co-CA) is added. This co-CA can be poly-(tetramethylene ether) glycol (1000 g mol⁻¹; DMC-PTMEG), polyethylene glycol (2000 g mol⁻¹; DMC-PEG) or Pluronic P123 triblock polymer (5750 g mol⁻¹; DMC-P123). Solution A is then stirred magnetically at 353 K. Solution B is prepared by dissolving 1 mmol of a metal cyanide salt K₃[Co(CN)₆] in 10 mL of deionized water. Solution B is added dropwise to solution A under vigorous stirring. After the addition, the mixture is left to stir for another 30 min at 353 K. Hereafter, 25 mL of the complexing agent (CA) ¹BuOH is added and the final mixture is stirred for another 3 h at 353 K. The synthesis can be repeated without addition of co-CA (DMC-X) or without addition of both CA and co-CA (DMC-pure). DMC-1:1 was also prepared without addition of CAs, but with equimolar amounts of Zn and Co. The resulting solids were centrifuged and washed three times with a 1:1 mixture of ¹BuOH and water. They are subsequently dried at 333 K overnight, followed by drying at 353 K under vacuum overnight.

*Reverse Emulsion Synthesis.*⁴⁰ Solution A was prepared by the addition of 10 g of Igepal CA-520 emulsifier and 7.7 mL of CA ¹BuOH to cyclohexane (109 mL) constituting the apolar phase. This solution was stirred at room temperature with a mechanical stirrer (300 rpm). Solution B was prepared by

dissolving 10 mmol of ZnCl₂ in 2 mL of deionized water, while solution C contained 2 mmol of K₃[Co(CN)₆] in 2 mL of deionized water. Solution B was first added dropwise to solution A under vigorous stirring. Next, solution C was added dropwise to the mixture, and left stirring for another hour at room temperature. The resulting particles were centrifuged and washed three times with ¹BuOH (NDMC-Igepal). The powder was then dried first at 333 K followed by drying at 353 K under vacuum overnight.

Instrumentation. XRD measurements were performed on a STOE Stadi MP operating in Bragg–Brentano mode. Measurements were carried out with CuKα radiation with a wavelength of 1.54060 Å using a linear position sensitive detector. SEM images were recorded on a Philips XL30 FEG after coating with a thin film of Au, followed by EDX recordings at 15 kV for chemical analysis. The EDX data were processed using EDAX software. IR measurements were performed on a Nicolet 6700 spectrometer using thin self-supporting wafers (±10 mg cm⁻²), prepared by application of pressure on the powder sample. The wafer was placed in a cell under vacuum and was heated to 448 K before an IR spectrum was recorded. The cell was cooled down to 323 K and pyridine was allowed to diffuse into the cell. Physisorbed pyridine was removed by heating up to 448 K under vacuum, before recording the IR spectrum. Nitrogen physisorption measurements were conducted at 77 K on a Quantachrome AS1Win instrument, after evacuation of the powder sample overnight at 373 K in vacuum. TGA measurements were carried out on a TGA Q500 of TA Instruments with a heating rate of 10 °C/min under O₂-atmosphere, in a high throughput mode. Zn and Co K-edge X-ray absorption spectra (XAS) were collected at B18 at the Diamond Light Source which operates at 3GeV. The beamline is equipped with Si(111) double crystal monochromator, ion chambers for measuring incident and transmitted beam intensity and a 9 element Ge fluorescence detector for measurement in fluorescence mode. All the measurements were carried out in fluorescence mode and typically 6 scans were averaged to produce the spectra. X-ray absorption spectra were processed using ATHENA⁵¹ software and subsequent analyses of the EXAFS data were performed using EXCURVE.⁵²

ASSOCIATED CONTENT

Supporting Information

General procedure for the catalysis experiments, ¹H NMR spectroscopic data, and GC-MS fragmentation data of all compounds. This material is available free of charge via the Internet at <http://pubs.acs.org>.

AUTHOR INFORMATION

Corresponding Author

*E-mail: dirk.devos@biw.kuleuven.be. Fax: (+32) 16 321 998.

Notes

The authors declare no competing financial interest.

ACKNOWLEDGMENTS

A.P. acknowledges the Fund for Scientific Research Flanders (FWO-Vlaanderen) and L'Oréal/UNESCO Belgium for financial support (Aspirant of FWO). D.E.D.V. thanks the Belgian Federal Government (IAP 7/05) and KU Leuven for the Methusalem CASAS grant. The authors thank the Diamond Light Source (U.K.) for beam time at the B18 beamline.

■ ABBREVIATIONS

DMC, double metal cyanide; CA, complexing agent; co-CA, cocomplexing agent; ^tBuOH, *tert*-butanol; PTMEG, poly-(tetramethylene ether) glycol; PEG, polyethylene glycol; P123, Pluronic P123; NDMC, nano double metal cyanide; Igepal, Igepal CA520; EXAFS, extended X-ray absorption fine structure

■ REFERENCES

- (1) Muller, T. E.; Hultsch, K. C.; Yus, M.; Foubelo, F.; Tada, M. *Chem. Rev.* **2008**, *108*, 3795–3892.
- (2) Brunet, J. J.; Neibecker, D. In *Catalytic Heterofunctionalization*; Togni, A., Grützmaier, H., Eds.; Wiley-VCH: Weinheim, Germany, 2001, p 91–141.
- (3) Hayes, K. S. *Appl. Catal., A* **2001**, *221*, 187–195.
- (4) Penzien, J. C.; Haessner, C.; Jentys, A.; Kohler, K.; Muller, T. E.; Lercher, J. A. *J. Catal.* **2004**, *221*, 302–312.
- (5) Shanbhag, G. V.; Halligudi, S. B. *J. Mol. Catal. A: Chem.* **2004**, *222*, 223–228.
- (6) Joseph, T.; Shanbhag, G. V.; Halligudi, S. B. *J. Mol. Catal. A: Chem.* **2005**, *236*, 139–144.
- (7) Shanbhag, G. V.; Halligudi, S. B. *Open Org. Chem. J.* **2008**, *2*, 52–57.
- (8) Lingaiah, N.; Babu, N. S.; Reddy, K. M.; Prasad, P. S. S.; Suryanarayana, I. *Chem. Commun.* **2007**, 278–279.
- (9) Yang, L.; Xu, L. W.; Xia, C. G. *Tetrahedron Lett.* **2008**, *49*, 2882–2885.
- (10) Mizuno, N.; Tabata, M.; Uematsu, T.; Iwamoto, M. *J. Catal.* **1994**, *146*, 249–256.
- (11) Lequette, M.; Figueras, F.; Moreau, C.; Hub, S. *J. Catal.* **1996**, *163*, 255–261.
- (12) Jimenez, O.; Muller, T. E.; Schwieger, W.; Lercher, J. A. *J. Catal.* **2006**, *239*, 42–50.
- (13) Motokura, K.; Nakagiri, N.; Mori, K.; Mizugaki, T.; Ebitani, K.; Jitsukawa, K.; Kaneda, K. *Org. Lett.* **2006**, *8*, 4617–4620.
- (14) Bhanushali, M. J.; Nandurkar, N. S.; Bhor, M. D.; Bhanage, B. M. *Catal. Commun.* **2008**, *9*, 425–430.
- (15) Qureshi, Z. S.; Deshmukh, K. M.; Tambade, P. J.; Dhake, K. P.; Bhanage, B. M. *Eur. J. Org. Chem.* **2010**, 6233–6238.
- (16) Liu, P. N.; Xia, F.; Zhao, Z. L.; Wang, Q. W.; Ren, Y. J. *Tetrahedron Lett.* **2011**, *52*, 6113–6117.
- (17) Richmond, M. K.; Scott, S. L.; Yap, G. P. A.; Alper, H. *Organometallics* **2002**, *21*, 3395–3400.
- (18) Tada, M.; Shimamoto, M.; Sasaki, T.; Iwasawa, Y. *Chem. Commun.* **2004**, 2562–2563.
- (19) Corma, A.; Gonzalez-Arellano, C.; Iglesias, M.; Navarro, M. T.; Sanchez, F. *Chem. Commun.* **2008**, 6218–6220.
- (20) Shanbhag, G. V.; Joseph, T.; Halligudi, S. B. *J. Catal.* **2007**, *250*, 274–282.
- (21) Duncan, C.; Biradar, A. V.; Asefa, T. *ACS Catal.* **2011**, *1*, 736–750.
- (22) Maurya, M. R.; Arya, A.; Kumar, U.; Kumar, A.; Avecilla, F.; Pessoa, J. C. *Dalton Trans.* **2009**, 9555–9566.
- (23) Zhao, J. Q.; Marks, T. J. *Organometallics* **2006**, *25*, 4763–4772.
- (24) Le Roux, E.; Liang, Y. C.; Storz, M. P.; Anwender, R. *J. Am. Chem. Soc.* **2010**, *132*, 16368–16371.
- (25) Hölderich, W.; Taglieber, V.; Pohl, H. H.; Kummer, R.; Baur, K. G. Process for amine manufacture. German Patent DE3634247C1, 1987.
- (26) Peeters, A.; Valvekens, P.; Vermoortele, F.; Ameloot, R.; Kirschhock, C.; De Vos, D. *Chem. Commun.* **2011**, *47*, 4114–4116.
- (27) Le-Khac, B.; Chester, W. Highly active double metal cyanide catalysts. U.S. Patent 5,714,428, 1998.
- (28) Hoffmann, J.; Ehlers, S.; Klinksiek, B.; Kluszczewski, B.; Steinlein, C.; Obendorf, L.; Pielartzik, H.; Pazos, J. F. Process for producing polyether polyols. U.S. Patent 2002/0198278 A1, 2002.
- (29) Ostrowski, T.; Ruppel, R.; Baum, S. Process for preparing polyether polyols. U.S. Patent 2006/223979 A1, 2006.
- (30) Huang, Y. J.; Qi, G. R.; Chen, L. S. *Appl. Catal., A* **2003**, *240*, 263–271.
- (31) Zhang, X. H.; Hua, Z. J.; Chen, S.; Liu, F.; Sun, X. K.; Qi, G. R. *Appl. Catal., A* **2007**, *325*, 91–98.
- (32) Lee, S. H.; Lee, I. K.; Ha, J. Y.; Jo, J. K.; Park, I.; Ha, C. S.; Suh, H.; Kim, I. *Ind. Eng. Chem. Res.* **2010**, *49*, 4107–4116.
- (33) Lee, I. K.; Ha, J. Y.; Cao, C.; Park, D. W.; Ha, C. S.; Kim, I. *Catal. Today* **2009**, *148*, 389–397.
- (34) Dienes, Y.; Leitner, W.; Muller, M. G. J.; Offermans, W. K.; Reier, T.; Reinholdt, A.; Weirich, T. E.; Muller, T. E. *Green Chem.* **2012**, *14*, 1168–1177.
- (35) Sreeprasanth, P. S.; Srivastava, R.; Srinivas, D.; Ratnasamy, P. *Appl. Catal., A* **2006**, *314*, 148–159.
- (36) Satyarthi, J. K.; Srinivas, D.; Ratnasamy, P. *Appl. Catal., A* **2011**, *391*, 427–435.
- (37) Saikia, L.; Satyarthi, J. K.; Gonnade, R.; Srinivas, D.; Ratnasamy, P. *Catal. Lett.* **2008**, *123*, 24–31.
- (38) Patil, M. V.; Yadav, M. K.; Jasra, R. V. *J. Mol. Catal. A: Chem.* **2007**, *273*, 39–47.
- (39) Sebastian, J.; Srinivas, D. *Chem. Commun.* **2011**, 47.
- (40) Yi, M. J.; Byun, S. H.; Ha, C. S.; Park, D. W.; Kim, I. *Solid State Ionics* **2004**, *172*, 139–144.
- (41) Mullica, D. F.; Milligan, W. O.; Beall, G. W.; Reeves, W. L. *Acta Crystallogr., Sect. B* **1978**, *34*, 3558–3561.
- (42) Wojdel, J. C.; Bromley, S. T.; Illas, F.; Jansen, J. C. *J. Mol. Model.* **2007**, *13*, 751–756.
- (43) Emeis, C. A. J. *Catal.* **1993**, *141*, 347–354.
- (44) Krap, C. P.; Zamora, B.; Reguera, L.; Reguera, E. *Microporous Mesoporous Mater.* **2009**, *120*, 414–420.
- (45) Autie-Castro, G.; Autie, M.; Reguera, E.; Santamaria-Gonzalez, J.; Moreno-Tost, R.; Rodriguez-Castellon, E.; Jimenez-Lopez, A. *Surf. Interface Anal.* **2009**, *41*, 730–734.
- (46) Krap, C. P.; Balmaseda, J.; del Castillo, L. F.; Zamora, B.; Reguera, E. *Energy Fuels* **2010**, *24*, 581–589.
- (47) Zboril, R.; Machala, L.; Mashlan, M.; Sharma, V. *Cryst. Growth Des.* **2004**, *4*, 1317–1325.
- (48) Natta, G.; Passerini, L. *Gazz. Chim. Ital.* **1929**, *59*, 620–642.
- (49) Kuyper, J.; Boxhoorn, G. *J. Catal.* **1987**, *105*, 163–174.
- (50) Rodriguez-Hernandez, J.; Reguera, E.; Lima, E.; Balmaseda, J.; Martinez-Garcia, R.; Yee-Madeira, H. *J. Phys. Chem. Solids* **2007**, *68*, 1630–1642.
- (51) Ravel, B.; Newville, M. *J. Synchrotron Radiat.* **2005**, *12*, 537–541.
- (52) Gurman, S. J.; Binsted, N.; Ross, I. *J. Phys. C: Solid State Phys.* **1984**, *17*, 143–151.